# Nonlinear transmission and light localization in photonic-crystal waveguides

**Sergei F. Mingaleev**

*Nonlinear Physics Group, Research School of Physical Sciences and Engineering, Australian National University, Canberra ACT 0200, Australia, and the Bogolyubov Institute for Theoretical Physics, 14-B Metrologichna, Kiev 03143, Ukraine*

**Yuri S. Kivshar**

*Nonlinear Physics Group, Research School of Physical Sciences and Engineering, Australian National University, Canberra ACT 0200, Australia*

Received January 15, 2002; revised manuscript received April 12, 2002; accepted April 19, 2002

We study light transmission in two-dimensional photonic-crystal waveguides with embedded nonlinear defects. First, we derive effective discrete equations with long-range interaction for describing the waveguide modes and demonstrate that they provide a highly accurate generalization of the familiar tight-binding models that are employed, e.g., for the study of coupled-resonator optical waveguides. Using these equations, we investigate the properties of straight waveguides and waveguide bends with embedded linear and nonlinear defects. We emphasize the role of evanescent modes in the transmission properties of such waveguides and demonstrate the possibility of the nonlinearity-induced bistable (all-optical switcher) and unidirectional (optical diode) transmission. Additionally, we demonstrate adaptability of our approach for investigation of multimode waveguides by the example of the bound states in their constrictions. © 2002 Optical Society of America

*OCIS codes:* 230.7370, 130.2790, 130.3120.

## 1. INTRODUCTION

Photonic crystals are usually viewed as an optical analog of semiconductors that modify the properties of light similarly to a microscopic atomic lattice that creates a semiconductor bandgap for electrons.[1] One of the most promising applications of photonic crystals is the possibility creating compact integrated optical devices,[2,3] which would be analogous to the integrated circuits in electronics but would operate entirely with light. Replacing relatively slow electrons with photons as the carriers of information can dramatically increase the speed and the bandwidth of advanced communication systems, thus revolutionizing the telecommunication industry.

To employ the high-technology potential of photonic crystals for optical applications and all-optical switching and waveguiding technologies, it is crucially important to achieve a dynamical tunability of their properties. For this purpose several approaches have been suggested (see, e.g., Ref. 4). One of the most promising concepts is based on the idea of employing the properties of nonlinear photonic crystals, i.e., photonic crystals made from dielectric materials whose refractive index depends on the light intensity. Exploration of the nonlinear properties of photonic bandgap materials is an important direction in current research that opens up a broad range of novel applications of photonic crystals for all-optical signal processing and switching, allowing an effective way to create highly tunable bandgap structures operating entirely with light.

One of the important concepts in the physics of photonic crystals is related to field localization on defects. In solid-state physics the idea of localization is associated with disorder that breaks the translational invariance of a crystal lattice and supports spatially localized modes with the frequency outside the phonon bands. A similar concept is well known in the physics of photonic crystals in which an isolated defect (a region of different refractive index that breaks periodicity) is known to support a localized defect mode. An array of such defects creates a waveguide that allows directed light transmission for the frequencies inside the band gap. Because the frequencies of the defect modes created by *nonlinear defects* depend on the electric field intensity, such modes can be useful in controlling light transmission. From the viewpoint of possible practical applications spatially localized states in optics can be associated with different types of all-optical switching devices in which light manipulates and controls light itself owing to the varying input intensity.

Nonlinear photonic crystals and photonic crystals with embedded nonlinear defects create an ideal environment for the observation of many of the nonlinear effects predicted earlier and studied in other branches of physics. In particular, the existence of nonlinear localized modes with the frequencies in the photonic bandgaps was already predicted and demonstrated numerically for several models of photonic crystals with the Kerr-type nonlinearity.[5–8]

In this paper, we study the resonant light transmission and localization in photonic-crystal waveguides and bends with embedded nonlinear defects. For simplicity,

we consider the case of a photonic crystal created by a square lattice of infinite dielectric rods, with waveguides made by the removal of some of the rods. Nonlinear properties of the waveguides are controlled by the embedding of the nonlinear defect rods. We demonstrate that the effective interaction in such waveguiding structures is nonlocal, and we suggest a novel, to our knowledge, theoretical approach that is based on effective discrete equations for describing both linear and nonlinear properties of such photonic-crystal waveguides and circuits, including the localized states at the waveguide bends. Additionally, we study the transmission of waveguide bends and emphasize the role of evanescent modes for the correct analysis of their properties.

The paper is organized as follows: In Section 2, we introduce our model of a two-dimensional (2-D) photonic crystal and provide a brief derivation of the effective discrete equations for the photonic-crystal waveguides (created by removed or embedded rods) that is based on the Green function technique. In Section 3, we apply these discrete equations to the analysis of the dispersion properties of straight waveguides. We also discuss a link between our approach and results obtained within the framework of the familiar tight-binding approximation often used in solid-state physics models. In Section 4, we demonstrate the applicability of our method for the study of the properties of multimode waveguides. As an example, we analyze the bound states in waveguide constriction. Sections 5 through 7 are devoted to the study of the transmission properties of straight waveguides and waveguide bends with embedded nonlinear defects. We emphasize the important role of evanescent modes that cannot be accounted for in the framework of the tight-binding model, which includes only the coupling between the nearest-neighbor defect modes. In particular, we demonstrate the possibility of bistable (Section 5) and unidirectional (Section 6) transmission and suggest that waveguide bends with embedded nonlinear defects can be employed for effective control of light transmission (Section 7). Section 8 concludes the paper with a summary of the results and discussions of the further applications of our approach.

## 2. EFFECTIVE DISCRETE EQUATIONS

In this section, we suggest and describe a novel theoretical approach based on effective discrete equations for describing many of the properties of the photonic-crystal waveguides and circuits, including the transmission spectra of sharp waveguide bends. This is an important part of our analysis because the properties of the photonic crystals and the photonic-crystal waveguides are usually studied by the solution of Maxwell's equations numerically, and such calculations are, generally speaking, time consuming. Moreover, the numerical solutions do not always provide good physical insight. The effective discrete equations that we derive below and employ further in the paper are somewhat analogous to the Kirchhoff equations for electric circuits. However, in contrast to electronics, in photonic crystals both diffraction and interference become important, and thus the resulting equations involve long-range interaction effects.

We introduce our approach for a simple model of 2-D photonic crystals consisting of infinitely long dielectric rods arranged in the form of a square lattice with a lattice spacing $a$. We study light propagation in the plane normal to the rods, assuming that the rods have a radius $r_0 = 0.18a$ and a dielectric constant of $\epsilon_0 = 11.56$ (this corresponds to GaAs or Si at a wavelength of $\sim 1.55$ $\mu$m). For the electric field $E(\mathbf{x}, t) = \exp(-i\omega t)E(\mathbf{x}|\omega)$ polarized parallel to the rods Maxwell's equations reduce to the eigenvalue problem

$$\left[\nabla^2 + \left(\frac{\omega}{c}\right)^2 \epsilon(\mathbf{x})\right] E(\mathbf{x}|\omega) = 0, \tag{1}$$

which can be solved by the plane-wave method.[9] A perfect photonic crystal of this type possesses a large (38%) TM bandgap between $\omega = 0.303(2\pi c/a)$ and $\omega = 0.444(2\pi c/a)$ (see Fig. 1), and it has been extensively employed during last few years for the study of bound states,[10] the transmission of light through sharp bends,[11,12] waveguide branches[13] and intersections,[14] channel drop filters,[15] nonlinear localized modes in straight waveguides,[7] and discrete spatial solitons in perfect 2-D photonic crystals.[8] Recently, this type of photonic crystal with a 90° bent waveguide was fabricated in macroporous silicon with $a = 0.57$ $\mu$m and a TM band gap at 1.55 $\mu$m.[16]

To create a waveguide circuit, we introduce a system of defects and assume, for simplicity, that the defects are identical rods of radius $r_d$ located at the points $\mathbf{x}_n$, where $n$ is the index number of the defect rods. Importantly, a similar approach can be employed equally well for the study of the defects created by the removal of isolated rods in a perfect 2-D lattice, and we demonstrate such examples below.

In a photonic crystal with defects the dielectric constant $\epsilon(\mathbf{x})$ can be presented as a sum of the periodic and the defect-induced terms, i.e., $\epsilon(\mathbf{x}) = \epsilon_p(\mathbf{x}) + \delta\epsilon(\mathbf{x})$, with

$$\delta\epsilon(\mathbf{x}) = \sum_n \epsilon_d[E(\mathbf{x}|\omega)] f(\mathbf{x} - \mathbf{x}_n), \tag{2}$$

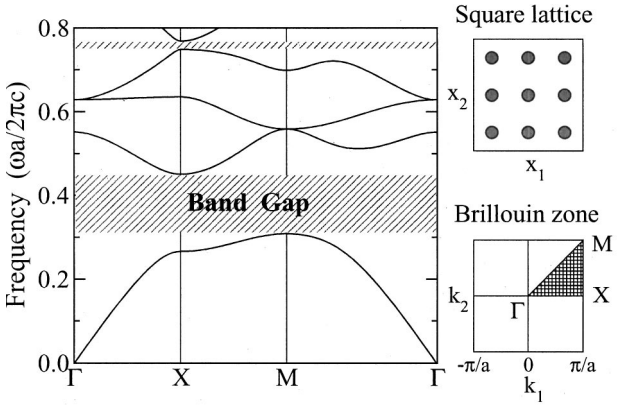


Fig. 1. Bandgap structure of the photonic crystal created by a square lattice of dielectric rods with $r_0 = 0.18a$ and $\epsilon_0 = 11.56$; the bandgaps are shown crosshatched. The top right-hand schematic shows a cross-sectional view of the 2-D photonic crystal. The bottom right-hand schematic shows the corresponding Brillouin zone with the irreducible zone shaded.

where $f(\mathbf{x}) = 1$ for $|\mathbf{x}| < r_d$ and vanishes otherwise. Equation (1) can be therefore written in the integral form

$$E(\mathbf{x}|\omega) = \left(\frac{\omega}{c}\right)^2 \int \mathrm{d}^2\mathbf{y} G(\mathbf{x}, \mathbf{y}|\omega)\,\delta\epsilon(\mathbf{y})E(\mathbf{y}|\omega), \qquad (3)$$

where $G(\mathbf{x}, \mathbf{y}|\omega)$ is the Green function of a perfect 2-D photonic crystal (see, e.g., Ref. 7).

A single defect rod is described by the function $\delta\epsilon(\mathbf{x}) = \epsilon_d f(\mathbf{x})$, and it can support one or more localized modes. Such localized modes are the eigenmodes of the discrete spectrum of the eigenvalue problem

$$\mathcal{E}_l(\mathbf{x}) = \left(\frac{\omega_l}{c}\right)^2 \int_{r_d} \mathrm{d}^2\mathbf{y} G(\mathbf{x}, \mathbf{y}|\omega_l)\epsilon_d f(\mathbf{y})\mathcal{E}_l(\mathbf{y}), \qquad (4)$$

where $\omega_l$ is the frequency (a discrete eigenvalue) of the $l$th eigenmode and $\mathcal{E}_l(\mathbf{x})$ is the corresponding electric field.

When we increase the number of defect rods (for example, to create photonic-crystal waveguide circuits),[11–15] the numerical solution of the integral equation (3) becomes complicated and, moreover, it is severely restricted by current computer capabilities. Therefore, one of our major goals in this paper is to describe the development of a new approximate physical model that would allow the application of fast numerical techniques, combined with a reasonably good accuracy, for the study of more complicated (linear and nonlinear) waveguide circuits in photonic crystals.

To achieve our goal, we consider the localized states created by a (in general, complex) system of defects [Eq. (2)] as a linear combination of the localized modes $\mathcal{E}_l(\mathbf{x})$ supported by isolated defects:

$$E(\mathbf{x}|\omega) = \sum_{l,n} \psi_n^{(l)}(\omega)\mathcal{E}_l(\mathbf{x} - \mathbf{x}_n). \qquad (5)$$

Substituting Eq. (5) into Eq. (3), multiplying it by $\mathcal{E}_{l'}(\mathbf{x} - \mathbf{x}_{n'})$, and integrating with $\mathbf{x}$, we obtain a system of discrete equations for the amplitudes $\psi_n^{(l)}$ of the $l$th eigenmodes localized at $n$th defect rods

$$\sum_{l,n} \lambda_{l,n}^{l',n'}\psi_n^{(l)} = \sum_{l,n,m} \epsilon_d \mu_{l,n,m}^{l',n'}(\omega)\psi_n^{(l)}, \qquad (6)$$

where

$$\lambda_{l,n}^{l',n'} = \int \mathrm{d}^2\mathbf{x}\mathcal{E}_l(\mathbf{x} - \mathbf{x}_n)\mathcal{E}_{l'}(\mathbf{x} - \mathbf{x}_{n'}),$$

$$\mu_{l,n,m}^{l',n'}(\omega) = \left(\frac{\omega}{c}\right)^2 \int \mathrm{d}^2\mathbf{x}\mathcal{E}_{l'}(\mathbf{x} - \mathbf{x}_{n'}) \times \int \mathrm{d}^2\mathbf{y} G(\mathbf{x}, \mathbf{y}|\omega) f(\mathbf{y} - \mathbf{x}_m)\mathcal{E}_l(\mathbf{y} - \mathbf{x}_n). \qquad (7)$$

It should be emphasized that the discrete equations (6) and (7) are derived by use of only the approximation provided by the ansatz equation (5). As can be demonstrated by a comparison of the approximate results with the direct numerical solutions of the Maxwell equations, this approximation is usually highly accurate, and it can be used in many physical problems.

However, the effective discrete equation (6) is still too complicated, and, in some cases, it can be simplified further and still remain accurate. A good example is the case of the photonic-crystal waveguides created by a sequence of widely separated defect rods. Such waveguides are known as *coupled-resonator optical waveguides*[17,18] (CROWs) or *coupled-cavity waveguides*.[19] For those cases, the localized modes located at each of the defect sites are only weakly coupled between themselves. As is known, such a situation can be described accurately by the so-called *tight-binding approximation* (see also Ref. 20). For our formalism this means that $\lambda_{l,n}^{l',nIH} = \mu_{l,n,m}^{l',n'} = 0$ for $|n' - n| > 1$ and $|n' - m| > 1$. The most important feature of the CROW circuits is that their bends are reflectionless throughout the entire band.[17,19] This nonreflection is in a sharp contrast to conventional photonic-crystal waveguides created by a sequence of removed or introduced defect rods (see, e.g., Ref. 11 and references therein) in which 100% transmission through a waveguide bend is known to occur only at certain resonant frequencies. In spite of this visible advantage, the CROW structures have a narrow guiding band, and, as a result, they also effectively demonstrate complete transmission through the waveguide bend in a narrow frequency interval.

Below, we consider different types of photonic-crystal waveguides and show that we provide an accurate simplification of Eq. (6) by accounting for *an indirect coupling* between the remote defect modes that is caused by the slowly decaying Green function, $\mu_{l,n,m}^{l',n'} \neq 0$ for $|n' - n| \leqslant L$, where the number $L$ of effectively coupled defects usually lies between five and ten. As we show below, this type of interaction, which is neglected in the tight-binding approximation, is important for understanding the transmission properties of the photonic-crystal waveguides. At the same time, we neglect a direct overlap between the nearest-neighbor eigenmodes, which is often considered to be important,[17,19] i.e., we consider $\lambda_{l,n}^{l',n'} = \delta_{l,l'}\delta_{n,n'}$ (with $\delta_{l,l'}$ being the Dirac delta function) and $\mu_{l,n,m}^{l',n'} = 0$ for $n \neq m$. Taking into account this interaction leads to negligible corrections only.

If we assume that the defects support only *the monopole eigenmodes* (marked by $l = 1$) the coefficients [Eqs. (7)] can be calculated reasonably accurately in the approximation that the electric field remains constant inside the defect rods, i.e., $\mathcal{E}_1(\mathbf{x}) \sim f(\mathbf{x})$. This relation corresponds to the averaging of the electric field in the integral equation (3) over the cross section of the defect rods.[7,21] In this case the resulting approximate discrete equation for the amplitudes of the electric fields $E_n(\omega) \equiv \psi_n{}^1(\omega)$ of the eigenmodes excited at the defect sites has the matrix form

$$\sum_m M_{n,m}(\omega)E_m(\omega) = 0,$$

$$M_{n,m}(\omega) = \epsilon_d(E_m)J_{n,m}(\omega) - \delta_{n,m}, \qquad (8)$$

where $J_{n,m}(\omega) \equiv \mu_{1,m,m}^{1,n}(\omega)$ is a coupling constant calculated in the approximation such that $\mathcal{E}_1(\mathbf{x}) \sim f(\mathbf{x})$, so

$$J_{n,m}(\omega) = \left(\frac{\omega}{c}\right)^2 \int_{r_d} \mathrm{d}^2\mathbf{y} G(\mathbf{x}_n, \mathbf{x}_m + \mathbf{y}|\omega) \qquad (9)$$

is completely determined by the Green function of a perfect 2-D photonic crystal (see details in Refs. 7 and 8).

First, we check the accuracy of our approximate model equation (8) for the case of *a single defect* located at the point $\mathbf{x}_0$. In this case, Eq. (8) yields the simple result $J_{0,0}(\omega_d) = 1/\epsilon_d$, and this expression defines the frequency $\omega_d$ of the defect mode. In particular, applying this result to the case when the defect is created by a single removed rod, we obtain the frequency $\omega_d = 0.391(2\pi c/a)$, which differs by only 1% from the value $\omega_d = 0.387(2\pi c/a)$, calculated with the help of the MIT Photonic-Bands numerical code.[9]

## 3. WAVEGUIDE DISPERSION

A simple single-mode waveguide can be created by the removal of a row of rods (see the inset in Fig. 2). Assuming that the waveguide is straight ($M_{n,m} \equiv M_{n-m}$) and neglecting the coupling between the remote defect rods (i.e., $M_{n-m} = 0$ for all $|n - m| > L$), we rewrite Eq. (8) in the transfer-matrix form, $\mathbf{F}_{n+1} = \hat{T}\mathbf{F}_n$, where we introduce the vector $\mathbf{F}_n = \{E_n, E_{n-1}, \ldots, E_{n-2L+1}\}$ and the transfer matrix $\hat{T} = \{T_{i,j}\}$ with the nonzero elements

$$T_{1,j}(\omega) = -\frac{M_{L-j}(\omega)}{M_L(\omega)}, \quad \text{for} \quad j = 1, 2, \ldots, 2L,$$

$$T_{j,j+1} = 1, \quad \text{for} \quad j = 1, 2, \ldots, 2L - 1. \qquad (10)$$

Solving the eigenvalue problem

$$\hat{T}(\omega)\mathbf{\Phi}^p = \exp\{ik_p(\omega)\}\mathbf{\Phi}^p, \qquad (11)$$

we can find the $2L$ eigenmodes of the photonic-crystal waveguide. The eigenmodes with real wave numbers $k_p(\omega)$ correspond to the modes propagating along the waveguide. In the waveguide shown in Fig. 2 there exist only two such modes (we denote them as $\mathbf{\Phi}^1$ and $\mathbf{\Phi}^2$), propagating in opposite directions ($k_1 = -k_2 > 0$). In Fig. 2, we plot the dispersion relation $k_1(\omega)$ calculated by

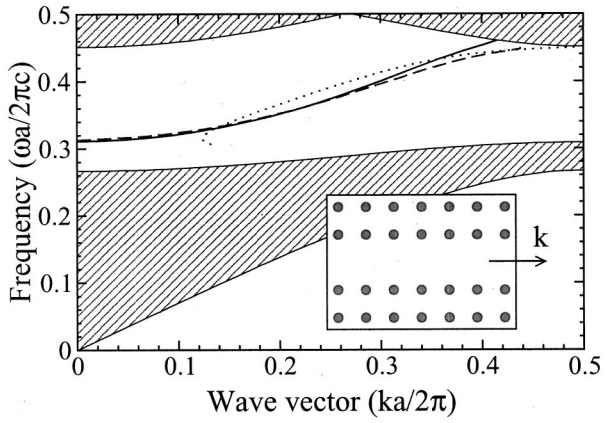


Fig. 2. Dispersion relation for a 2-D photonic-crystal waveguide (shown in the inset) as calculated by the supercell method[9] (solid curve) and from approximate equations (10) and (11) for $L = 7$ (dashed curve) and $L = 1$ (dotted curve). The hatched areas are the projected band structure of a perfect 2-D crystal.

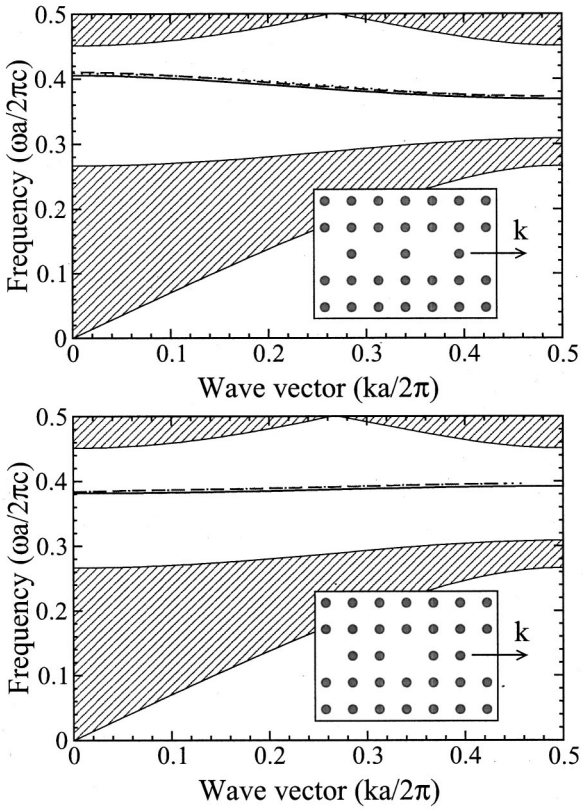


Fig. 3. Same as for Fig. 2 but for two other types of waveguides better described by the tight-binding models. The solid curve represents results from supercell calculations; the dotted and the dashed curves represent results from the approximate equations.

*three different methods*: The first method (solid curve) is calculated directly by the supercell approach,[9] whereas those for the dotted and the dashed curves are found from Eq. (11) in the nearest-neighbor approximation ($L = 1$; dotted curve) and also when we take into account the long-range interaction through the coupling between several neighbors ($L = 7$; dashed curve). As soon as the long-range interaction is taken into account, we observe a very good agreement between the results provided by our effective discrete equations and those obtained by the supercell method, except for a narrow region of large frequencies, where the dispersion curve penetrates into the spectrum band. The discrepancy in this latter region appears to be due to coupling between localized defect modes and extended band modes in the vicinity of the band edge, the effect of which is beyond the approximation of the discrete equations.

It is important to emphasize that the well-known *tight-binding approximation* that includes coupling between the nearest-neighbor defects only (i.e., $L = 1$) is not valid for the waveguide shown in Fig. 2. Generally speaking, the interaction between remote rods cannot be neglected as soon as we study the waveguides created by the removal (or the insertion) of the rods along a row or more complicated structures of this type. In such a case, as can be seen from Fig. 2, the dispersion relation found in the tight-binding approximation is incorrect, and, to obtain accurate results, one should take into account the coupling between several defect rods.

However, for the waveguides of a different geometry when only the second (or the third, etc.) rods are removed all methods provide reasonably good agreement with the direct numerical results, as is shown for two examples in Fig. 3. In this case, the waveguides are created by *an array of weakly coupled cavity modes*, and they are similar to the CROW structures analyzed earlier by several authors.[17–19] Thus the dispersion properties of CROWs (or similar waveguides) can be described with good accuracy by the tight-binding approximation; our new approach confirms this conclusion, and it provides a simple method for the derivation of the approximate equations and estimation of its validity.

## 4. BOUND STATES AND MULTIMODE WAVEGUIDES

As is well known (see, e.g., Ref. 10), photonic-crystal waveguides with embedded defects (as well as waveguide bends, branches, intersections, etc.) can support *localized bound modes* with the frequencies inside the bandgaps. Our approach permits the study of such bound states as localized solutions (localized eigenmodes) of the effective discrete equation (8).

Recently, we showed that Eq. (8) describes, with an accuracy of 1.5%, the bound states supported by a 90° waveguide bend.[22] Here, we provide a different example and consider a multimode waveguide formed by the removal of four rows of rods in the (11) direction of the lattice. Specifically, to provide a comparison with the case studied by direct numerical approach, we take the example studied earlier in Ref. 10. Such a waveguide supports *four guided modes* that repel each other, creating a bandgap in the interval $\omega = 0.390(2\pi c/a)$ to $\omega = 0.417(2\pi c/a)$ (Ref. 10). First, we solve Eq. (8) by taking into account the coupling between the $L = 7$ neighbors and recover the waveguide bandgap in the interval between $\omega = 0.387(2\pi c/a)$ to $\omega = 0.410(2\pi c/a)$ with an accuracy of approximately 1.7%. Introducing a narrow constriction into this multimode waveguide, as is shown in Fig. 4, we create a defect that can support *five localized bound states* with the frequencies inside the waveguide bandgap. One of these modes [depicted in Fig. 4(c)] was found and discussed in more detail earlier in Ref. 10 (see Fig. 5 from the cited paper). Such a mode was calculated in Ref. 10 for a photonic crystal with $r = 0.12a$, and thus the frequency of the bound state found there differs slightly from our result. It was shown that, in some simple cases, when a waveguide constriction (or a waveguide bend) can be considered as a finite section of a waveguide of a different type, the bound states correspond closely to the cavity modes excited in this finite section. However, such a simplified one-dimensional model does not correctly describe more complicated cases,[10] even the properties of a simple waveguide bend discussed in Ref. 22. The situation becomes even more complicated for waveguide branches.[13] In contrast, solving the discrete equation (8), we can find the frequencies and the profiles of the bound states excited in an arbitrary complex set of defects.

## 5. RESONANT TRANSMISSION OF AN ARRAY OF DEFECTS

In addition to the propagating guided modes, in photonic-crystal waveguides there always exist *evanescent modes* with imaginary $k_p$. These modes cannot be accounted for within the framework of the tight-binding theory that relies on the nearest-neighbor interaction between defect rods. However, we can find evanescent modes in an extended discrete model equation (8) by taking into account coupling between several neighboring defects. To illus-

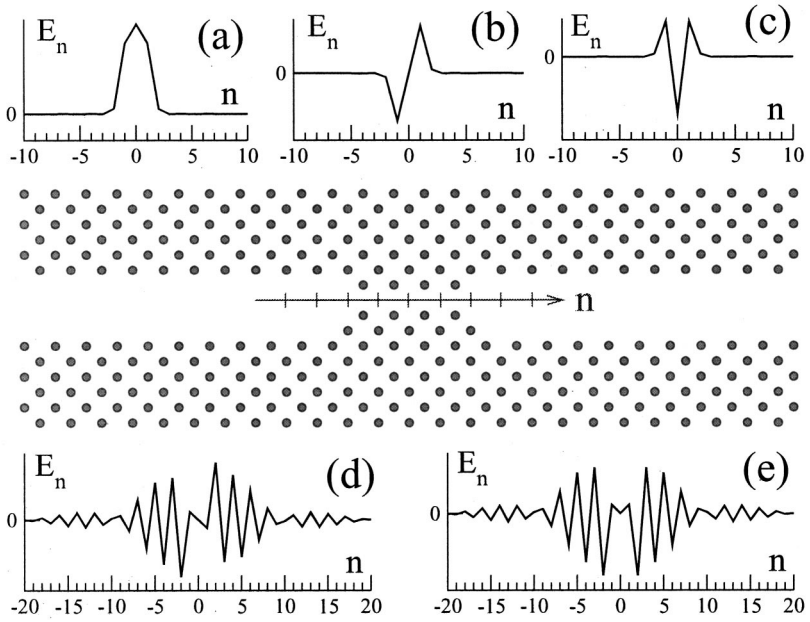


Fig. 4. Electric field $E_n$ for five bound states supported by the multimode waveguide with the constriction shown in the center. The center of the constriction is located at $n = 0$. The frequencies ($\omega a/2\pi c$) of the bound states are (a) 0.389, (b) 0.391, (c) 0.392, (d) and (e) 0.402.

trate this statement, we plot, in Fig. 5, on a complex plane all 14 eigenmodes found for $L = 7$ from Eq. (11) for the waveguide shown in Fig. 2. As we can see from that plot, the imaginary parts of $k_p$ for all evanescent modes are between 1.09 and 1.18. This outcome means that such modes decay rather slowly, and they should manifest themselves in various phenomena of the waveguide transmission and localized modes. Moreover, they decay almost equally slowly, and thus, to obtain accurate results, we should account for them all. That is why in our calculations we include the coupling between the $L = 7$ neighbors. For smaller $L$, we may lose the effects associated with some of the evanescent modes. For larger values of $L$ there appear new evanescent modes that, however, decay quite rapidly and can therefore be neglected.

Although the evanescent modes remain somewhat hidden in straight waveguides, they become crucially important in more elaborate structures such as waveguides with embedded linear or nonlinear defects and waveguide bends and branches. In these cases the evanescent modes manifest themselves in several different ways. In particular, they determine *nontrivial transmission properties* of the photonic-crystal circuits considered below.

As a first example of the application of our approach, we study the transmission of a straight waveguide with embedded nonlinear defects. Such a structure can be considered to be two semi-infinite straight waveguides coupled by a finite region of defects located between them. The coupling region may include both linear (as a domain of a perfect waveguide) and nonlinear (embedded) defects. We assume that the defect rods inside the coupling region are characterized by the index that runs from $a$ to $b$ and that the amplitudes $E_m$ $(m = a, \ldots, b)$ of the electric field at the defects are all unknown. We number the guided modes of Eq. (11) in the following way: $p = 1$ corresponds to the mode propagating in the direction of the nonlinear section (for both ends of the waveguide), $p = 2$, corresponds to the mode propagating in the opposite direction, $p = 3, \ldots, L + 1$ corresponds to the evanescent modes that grow in the direction of the nonlinear section, and $p = L + 2, \ldots, 2L$ corresponds to the evanescent modes that decay in the direction of the nonlinear section. Then we can write the incoming and the outgoing waves in the semi-infinite waveguide sections as a superposition of the guided modes:

$$E_m^{\text{in}} = \alpha_i \Phi_{a-m}{}^1 + \alpha_r \Phi_{a-m}{}^2 + \sum_{p=3}^{L+1} \beta_p{}^{\text{in}} \Phi_{a-m}{}^p, \quad (12)$$

for $m = a - 2L, \ldots, a - 1$, and

$$E_m^{\text{out}} = \alpha_t \Phi_{m-b}{}^2 + \sum_{p=3}^{L+1} \beta_p{}^{\text{out}} \Phi_{m-b}{}^p, \quad (13)$$

for $m = b + 1, \ldots, b + 2L$, where $\beta_p{}^{\text{in}}$ and $\beta_p{}^{\text{out}}$ are unknown amplitudes of the evanescent modes growing in the direction of the nonlinear section, whereas $\alpha_i$, $\alpha_t$, and $\alpha_r$ are unknown amplitudes of the incoming, the transmitted, and the reflected, respectively, propagating waves. We take into account that the evanescent modes with $p > L + 1$ (growing in the directions of the waveguide ends) must vanish. Now, substituting Eqs. (12) and (13) into Eq. (8), we obtain a system of linear (or nonlinear for nonlinear defects) equations with $2L + b - a + 1$ unknown. Solving this system, we find the transmission coefficient, $T = |\alpha_t/\alpha_i|^2$, and the reflection coefficient, $R = |\alpha_r/\alpha_i|^2$, as functions of the light frequency $\omega$ and the intensity $|\alpha_i|^2$ or $|\alpha_t|^2$. Recently, we demonstrated[22] that the linear transmission properties of the waveguide bends are described accurately by this approach. Below, we study *nonlinear transmission* of the photonic-crystal waveguides and waveguide bends.

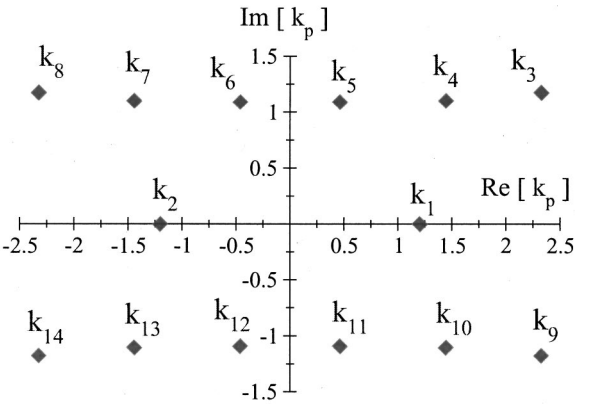


Fig. 5. Wave vectors $k_p(\omega)$ for $\omega = 0.351$ found by use of Eq. (11) for the waveguide shown in Fig. 2 (with $a = 1$).

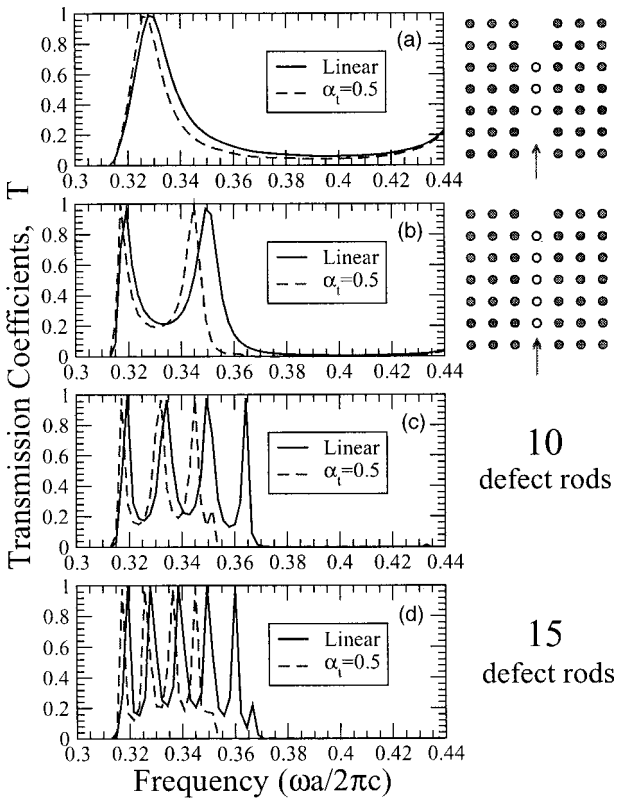


Fig. 6. Transmission coefficients of an array of nonlinear defect rods calculated from Eqs. (8)–(13) with $L = 7$ in the linear limit of very small $|\alpha_t|^2$ (solid curves) and for nonlinear transmission when the output intensity is $|\alpha_t|^2 = 0.25$ (dashed curves), for different numbers of the defects. We use nonlinear defect rods with the dielectric constant $\epsilon_d^{(0)} = 7$; they are marked by open circles on the diagrams on the right-hand side.

In Fig. 6, we present our results for the transmission spectra of straight waveguides (created by a row of removed rods) with an array of embedded nonlinear defects. We assume throughout the paper that all nonlinear defect rods are identical, with a radius of $r_d = r_0 = 0.18a$ and a dielectric constant of $\epsilon_d = \epsilon_d^{(0)} + |E_n|^2$ [with $\epsilon_d^{(0)} = 7$], which grows linearly with the light intensity (the so-called Kerr effect). In the linear limit, the embedded defects behave like an effective resonant filter, and only the waves with some specific resonance frequencies can effectively be transmitted through the defect section. The resonances appear to be due to the excitation of cavity modes inside the defect region, whereas a single defect does not demonstrate any resonant behavior. When the intensity of the input wave grows the resonant frequencies found in the linear limit are shifted to lower values. The sensitivity of different resonances to the change in light intensity is quite different and may be tuned by our matching the defect parameters. Nonlinear resonant transmission is found to possess *bistability*, similarly to another problem of the nonlinear transmission (see, e.g., Refs. 23–25). Bistable transmission occurs for frequencies smaller than the resonant, in a linear limit, frequency (see Fig. 7).

## 6. OPTICAL DIODE

An all-optical diode is a spatially nonreciprocal device that allows unidirectional propagation of a signal at a given wavelength. In the ideal case, the diode transmission is 100% in the forward propagation, whereas it is much smaller or vanishes for backward (opposite) propagation, yielding a unitary contrast.

The first study of the operational mechanism for a passive optical diode based on a photonic bandgap material was carried out by Scalora and co-workers.[26,27] These authors considered the pulse propagation near the band edge of a one-dimensional photonic-crystal structure with a spatial gradation in the linear refractive index, together with a nonlinear medium response, and found that such a structure can result in unidirectional pulse propagation.

To implement this concept for the waveguide geometry discussed in Section 5, we consider an asymmetric structure made up of four nonlinear defect rods, as shown in the diagrams on the right-hand side in Fig. 8. Figure 8

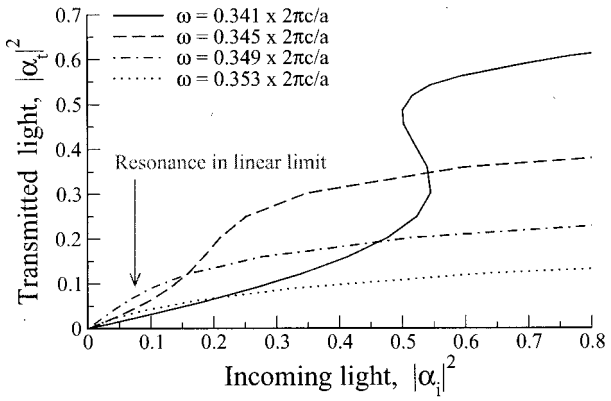


Fig. 7. Bistability in the nonlinear transmission of an array of five nonlinear defect rods shown in Fig. 6(b).

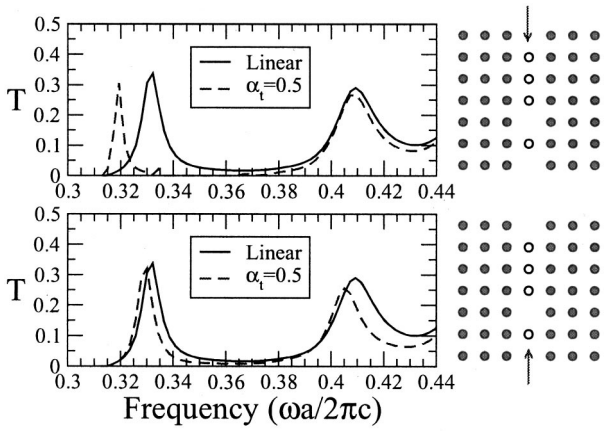


Fig. 8. Transmission coefficients of an asymmetric array of nonlinear defect rods calculated for the same parameters as in Fig. 6.

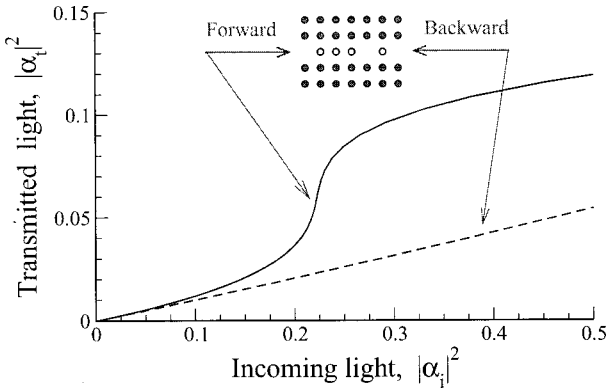


Fig. 9. Nonlinear transmission of the optical diode for the forward (see top of Fig. 8) and the backward (see bottom of Fig. 8) directions at a light frequency of $\omega = 0.326(2\pi c/a)$.

shows the transmission spectra of such an asymmetric structure in the opposite directions indicated by the two arrows in diagrams on the right-hand side. As can be seen, in the linear limit the transmission is characterized by two resonant frequencies and does not depend on the propagation direction. However, because the sensitivity of both resonant frequencies to the change in the light intensity is different for the forward (see Fig. 8, top) and the backward (see Fig. 8, bottom) propagation directions, the transmission becomes, in the vicinity of resonant frequencies, highly asymmetric for large input intensities. This asymmetry results in nearly unidirectional waveguide transmission, as is shown in Fig. 9.

In contrast to the perfect resonators used for Fig. 6, the transmission of the asymmetric structure under consideration is not very efficient at the resonant frequencies. However, we expect that the optical diode effect, with much better efficiency, can be found in other types of waveguide geometry and that a unitary contrast can be achieved by proper optimization of the waveguide and the defect parameters, which can be carried out by use of our method and the effective discrete equations derived in Section 2.

## 7. WAVEGUIDE BENDS

As one of the final examples in this paper, we study the transmission properties of waveguide bends. We con-

sider a bent waveguide as consisting of two coupled semi-infinite straight waveguides with a finite section of defects between them. The finite section includes a bend with a safety margin of the straight waveguide at both ends. Similar to what we discussed in Section 5 for straight waveguides, we can solve the system of effective discrete equations to find the transmission, $T = |\alpha_t/\alpha_i|^2$, and the reflection, $R = |\alpha_r/\alpha_i|^2$, coefficients of the waveguide bends. In Fig. 10, we present our results for the transmission spectra of several types of bent waveguides, which were discussed in Ref. 11, where the possibility of high transmission through sharp bends in photonic-crystal waveguides was first demonstrated. We compare the reflection coefficients calculated by the finite-difference time-domain method in Ref. 11 (dashed curves) with our results, calculated from Eqs. (8)–(13) for $L = 7$ (solid curves) and for $L = 2$ (dotted curve in the top plot). As can clearly be seen, Eqs. (8)–(13) provide a very accurate method for calculating the transmission spectra of waveguide bends, if only we account for long-range interactions. It should be emphasized that the approximation in which only next-neighbor interactions are taken into account is usually too crude, whereas the tight-binding theory incorrectly predicts perfect transmission for all guiding frequencies.

The resonant transmission can be modified dramatically by the insertion of both linear and nonlinear defects into the waveguide bends. To illustrate such features, we consider the waveguide bend with three embedded nonlinear defects, as is depicted in Fig. 11 in the right-hand-side diagram, where these defects are shown by open circles. In the linear regime such a sharp bend behaves as an optical threshold device that efficiently transmits the guided waves with frequencies above the threshold frequency but completely reflects the waves with the lower frequencies. The transmission coefficient of this waveguide bend in the linear limit is shown in Fig. 11 by a solid curve. When the input intensity increases the threshold frequency decreases, extending the transmission region (see the dashed curve in Fig. 11). The resulting transmission plotted as a function of the input intensity demonstrates a sharp nonlinear threshold character with extremely low transmission of the waves below a certain (rather small) threshold intensity (see Fig. 12).

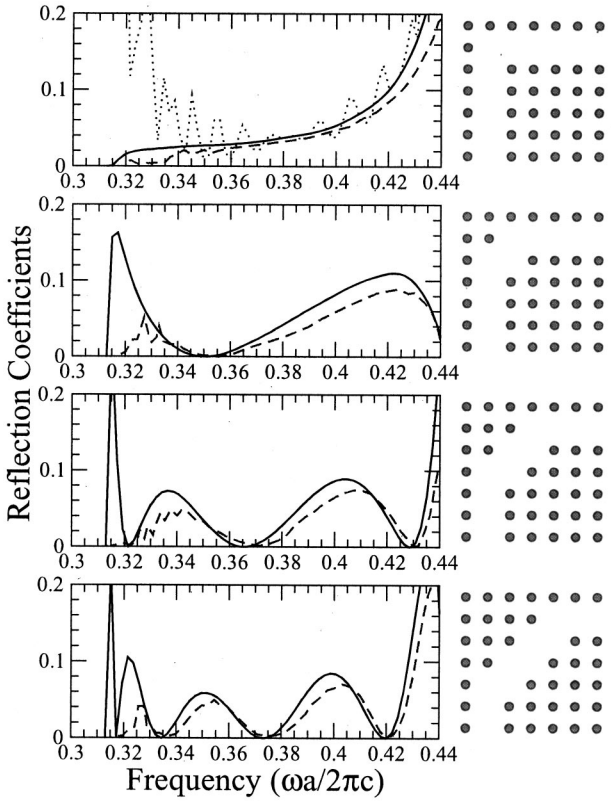


Fig. 10. Reflection coefficients calculated by the finite-difference time-domain method (dashed curve; from Ref. 11) and from Eqs. (8)–(13) with $L = 7$ (solid curves) and $L = 2$ (dotted curve; only in the top plot) for different bend geometries.

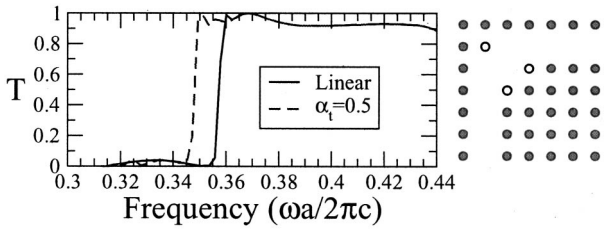


Fig. 11. Transmission of a waveguide bend with three embedded nonlinear defect rods in the linear (solid curve) and the nonlinear (dashed curve) regimes. The defect rods have a dielectric constant of $\epsilon_d^{(0)} = 7$, and they are marked by open circles.

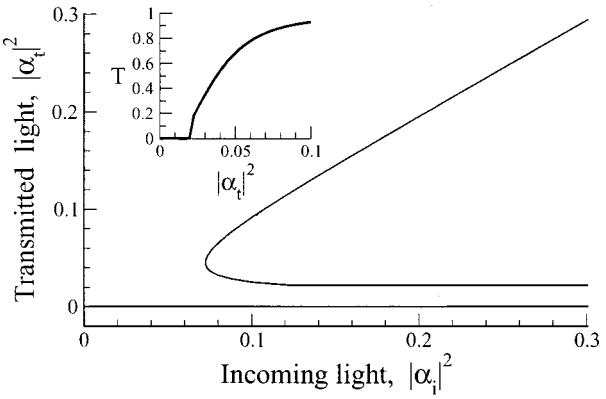


Fig. 12. Bistable nonlinear transmission through the waveguide bend shown in Fig. 11, for a light frequency of $\omega = 0.351(2\pi c/a)$.

## 8. CONCLUSIONS

We have suggested a novel conceptual approach for describing a broad range of transmission properties of photonic-crystal waveguides and circuits. Our approach is based on the analysis of the effective discrete equations derived with the help of the Green function technique, and it generalizes the familiar tight-binding approximations that are usually employed to study CROWs or coupled-cavity optical waveguides. The effective discrete equations that we have introduced in this paper emphasize the important role played by the evanescent modes in the transmission characteristics of photonic-crystal circuits with waveguide bends and embedded defects. Employing this technique, we have studied the properties of

several important elements of (the linear and the nonlinear) photonic-crystal circuits, including a nonlinear bistable transmitter and an optical diode created by an asymmetrical structure of nonlinear defects. We believe that our approach can be useful for solving more complicated problems and that it can be applied to study transmission characteristics of waveguide branches and channel drop filters.

## ACKNOWLEDGMENTS

We thank J. D. Joannopoulos and S. Soljačić for encouraging comments and discussions. This research was partially supported by the Australian Research Council and the Performance and Planning Found of the Australian National University.

## REFERENCES

1. J. D. Joannoupoulos, R. B. Meade, and J. N. Winn, *Photonic Crystals: Molding the Flow of Light* (Princeton U. Press, Princeton, N.J., 1995).
2. K. Sakoda, *Optical Properties of Photonic Crystals* (Springer-Verlag, Berlin, 2001).
3. T. F. Krauss and R. M. De la Rue, "Photonic crystals in the optical regime—past, present and future," Prog. Quantum Electron. **23**, 51–96 (1999), and references therein.
4. See, e.g., K. Busch and S. John, "Liquid-crystal photonic-band-gap materials: the tunable electromagnetic vacuum," Phys. Rev. Lett. **83**, 967–970 (1999), and discussions therein.
5. S. John and N. Aközbek, "Nonlinear optical solitary waves in a photonic band gap," Phys. Rev. Lett. **71**, 1168–1171 (1993).
6. S. John and N. Aközbek, "Optical solitary waves in two- and three-dimensional nonlinear photonic band-gap structures," Phys. Rev. E **57**, 2287–2319 (1998).
7. S. F. Mingaleev, Yu. S. Kivshar, and R. A. Sammut, "Long-range interaction and nonlinear localized modes in photonic crystal waveguides," Phys. Rev. E **62**, 5777–5782 (2000).
8. S. F. Mingaleev and Yu. S. Kivshar, "Self-trapping and stable localized modes in nonlinear photonic crystals," Phys. Rev. Lett. **86**, 5474–5477 (2001).
9. S. G. Johnson and J. D. Joannopoulos, "Block-iterative frequency-domain methods for Maxwell's equations in a plane-wave basis," Opt. Express **8**, 173–190 (2001), http://epubs.osa.org//optics.express.
10. A. Mekis, S. H. Fan, and J. D. Joannopoulos, "Bound states in photonic crystal waveguides and waveguide bends," Phys. Rev. B **58**, 4809–4817 (1998).
11. A. Mekis, J. C. Chen, I. Kurland, S. H. Fan, P. R. Villeneuve, and J. D. Joannopoulos, "High transmission through sharp bends in photonic crystal waveguides," Phys. Rev. Lett. **77**, 3787–3790 (1996).
12. S. Y. Lin, E. Chow, V. Hietala, P. R. Villeneuve, and J. D. Joannopoulos, "Experimental demonstration of guiding and bending of electromagnetic waves in a photonic crystal," Science **282**, 274–276 (1998).
13. S. Fan, S. G. Johnson, J. D. Joannopoulos, C. Manolatou, and H. A. Haus, "Waveguide branches in photonic crystals," J. Opt. Soc. Am. B **18**, 162–165 (2001).
14. S. G. Johnson, C. Manolatou, S. Fan, P. R. Villeneuve, J. D. Joannopoulos, and H. A. Haus, "Elimination of cross talk in waveguide intersections," Opt. Lett. **23**, 1855–1857 (1998).
15. S. H. Fan, P. R. Villeneuve, and J. D. Joannopoulos, "Channel drop tunneling through localized states," Phys. Rev. Lett. **80**, 960–963 (1998).
16. T. Zijlstra, E. van der Drift, M. J. A. de Dood, E. Snoeks, and A. Polman, "Fabrication of two-dimensional photonic crystal waveguides for 1.5 $\mu$m in silicon by deep anisotropic dry etching," J. Vac. Sci. Technol. B **17**, 2734–2739 (1999).
17. A. Yariv, Y. Xu, R. K. Lee, and A. Scherer, "Coupled-resonator optical waveguide: a proposal and analysis," Opt. Lett. **24**, 711–713 (1999).
18. Y. Xu, R. K. Lee, and A. Yariv, "Propagation and second-harmonic generation of electromagnetic waves in a coupled-resonator optical waveguide," J. Opt. Soc. Am. B **17**, 387–400 (2000).
19. M. Bayindir, B. Temelkuran, and E. Ozbay, "Propagation of photons by hopping: a waveguiding mechanism through localized coupled cavities in three-dimensional photonic crystals," Phys. Rev. B **61**, R11855–R11858 (2000).
20. E. Lidorikis, M. M. Sigalas, E. Economou, and C. M. Soukoulis, "Tight-binding parametrization for photonic band gap materials," Phys. Rev. Lett. **81**, 1405–1408 (1998).
21. A. R. McGurn, "Green's-function theory for row and periodic defect arrays in photonic band structures," Phys. Rev. B **53**, 7059–7064 (1996).
22. S. F. Mingaleev and Yu. S. Kivshar, "Effective equations for photonic crystal waveguides and circuits," Opt. Lett. **27**, 231–233 (2002).
23. F. Delyon, Y.-E. Lévy, and B. Souillard, "Nonperturbative bistability in periodic nonlinear media," Phys. Rev. Lett. **57**, 2010–2013 (1986).
24. Q. Li, C. T. Chan, K. M. Ho, and C. M. Soukoulis, "Wave propagation in nonlinear photonic band-gap materials," Phys. Rev. B **53**, 15577–15585 (1996).
25. E. Centero and D. Felbacq, "Optical bistability in finite-size nonlinear bidimensional photonic crystals doped by a microcavity," Phys. Rev. B **62**, R7683–R7686 (2000).
26. M. Scalora, J. R. Dowling, C. M. Bowden, and M. J. Bloemer, "The photonic band edge optical diode," J. Appl. Phys. **76**, 2023–2026 (1994).
27. M. D. Tocci, M. J. Bloemer, M. Scalora, J. P. Dowling, and C. M. Bowden, "Thin-film nonlinear optical diode," Appl. Phys. Lett. **66**, 2324–2326 (1995).